ISSN 2321-807X
Volume 13 Number6
Journal of Advances in chemistry

Electronic Properties and Vibratational Analysis of Synthesized g-C3N4 nanoparticles using Density Functional Theory

R. Nithya [a], S. Ayyappan[a*], M. Saranya[a], R.K. Sangeetha[b], S. Gokila[b]
[a,a*]Department of Physics, Government College of Technology, Coimbatore, India.
[b]Department of Physics, Sri Eshwar College of Engineering, Coimbatore, India.
Corresponding author - Dr. S. Ayyappan E-mail: ayyappan@gct.ac.in

Abstract

In the present work, Polymeric metal free Graphitic carbon nitride (g-C_3N_4) nano particle was synthesized by thermal pyrolysis method without any additives or surfactants. XRD and SEM micrographs clearly show the formation of hexagonal phase of the as prepared g-CN nanoparticles. Calculated FT-IR, FT-Raman and UV-Vis spectra of the g-CN have been analyzed. HOMO LUMO and density of states of the title compound were calculated by density functional theory. Hyper polarizability of the graphitic carbon nitride was calculated by Hartee Fock and density functional method at 6-31G (d,p) basis set. The Natural bonding orbital of graphitic carbon nitride were analysed.

Keywords: metal free g-C_3N_4, UV-Visible, DFT, HOMO-LUMO, Hyper polarizability, NBO, MEP mapping.

1. INTRODUCTION

Graphitic carbon nitride materials are compounds that are very similar to graphite, the “mother compound” of graphene, and therefore promising candidates for the formation of 2D materials with outstanding properties and graphite-like structure [1]. Graphite-like carbon nitride networks have recently gained significant interest regarding their exceptional chemical stability and their manifold properties [2]. Due to the special electron structures, carbon nitride is a kind of novel organic and metal-free semiconductors [3]. Owing to their special properties such as the super hardness, low density, reliable chemical inertness, water resistivity, wear resistance and biocompatibility, carbon nitride was regarded as the promising materials applied in the emission devices, surface modification, medical science and photocatalysis, etc. As an analogue of graphite, graphitic carbon nitride (g-C_3N_4) polymer with band gap of 2.7 eV is the most stable allotrope of carbon nitride possessing a stacked two-dimensional structure in the ambient conditions [2]. It is composed of only carbon and nitrogen which is stable in acidic and basic medium due to the strong covalent bond between carbon and nitrogen atoms [4]. Moreover, the most important is that we can handle the band gap of carbon nitride via doping or modification of its morphology.

Density Functional Theory methods are used to investigate the structures and relative energetics of sp^2 and sp^3 bonded carbon nitride solids [4]. Different structural forms of C_3N_4 have been predicted including α-C_3N_4, β-C_3N_4, graphitic-C_3N_4 (g- C_3N_4), pseudo cubic- C_3N_4 (bl- C_3N_4) and cubic- C_3N_4 [5]. Among these phases, the Graphitic carbon nitride is the most stable structure. The unit cell contains 14 atoms and exhibits P6m2 symmetry [6]. The bonding in C_3N_4 is important for characterization and identification of the material. The material will have carbon four-coordinated with nitrogen (sp^3 hybridised) and nitrogen three-coordinated with carbon. Recently, Gracia et al [7] has investigated on g-CN nanotubes based on DFT calculations. Koh et al.[8] have used DFT to show that Carbon nitride nanotubes are attractive towards nitrogen. Due to the N content in of g-C_3N_4, there is a periodic distribution of pores. According to their distribution, there are two different allotropic structures: triazine and tri-s-triazine. By means of DFT calculations, Teter et al [8] studied the different allotropic forms of C_3N_4. About triazine, they found that the layers are stacked on AB type with a unit cell of 14 atoms.

In this work, we report the experimental and theoretical studies of Graphitic carbon nitride (g-CN) with an insight on the physicochemical properties and their chemical reactivity. The experimental FTIR, Raman, UV spectra of pristine g-CN at room temperature and assigning vibrational frequencies using density functional theory calculations were investigated. In addition, HOMO and LUMO analyses have been calculated toelucidate the information regarding charge transfer within the molecule.

2. EXPERIMENTAL STUDIES

2.1. Synthesis of g-C_3N_4Nanoparticles

In the present work, g-C_3N_4 nanoparticles were prepared by directly treating thiourea at 450◦C for 3 h in air. The precursor is easily available in the chemical industry at low cost.In a typical synthesis, 10 g of thiourea was put into a closed alumina crucible with a cover and then heated to 450◦C in a muffle furnace for 3 h at a heating rate of 10◦Cmin^{-1}. After the reaction, the alumina crucible was cooled to room temperature. The resultant g-C_3N_4 were collected and ground into powder, respectively.

2.2. Experimental Details

The graphitic carbon nitride nanoparticle in yellow color solid form was synthesized by thermal pyrolysis method. X-ray diffraction (XRD) patterns were recorded at room temperature at the scanning rate of 0.02°/min for the range from 10° – 90° using P analytical X'Pert-Pro diffractometer with Cu $K\alpha_1$ radiation (λ=1.5406 A°). The UV-visible spectrum was recorded in the range of 200- 900 nm using a JoscoV-650 spectrophotometer.The Fourier transform infrared spectra of the

GCN nanocompounds were obtained by using a Fourier transform infrared (FTIR) spectrometer (Bruker Tensor 27, Germany) with an operating range of 400 cm^{-1}- 4000 cm^{-1} in a KBr pellet technique using the excitation wavelength of 1064nmspectral line of Nd-YAG laser. The Fourier transform Raman spectra were obtained with a range of 4000 cm^{-1}-400 cm^{-1} recorded using JY-1058 Raman spectrometer with excitation wavelength of 532 nm laser source.

2.3. Computational Details

The entire Quantum chemical calculations were done by Density functional theory(DFT) by B3LYP method using Gaussian 09 program package. The initial Geometrical structure generated from the geometrical parameters was minimized without any constrains in the potential energy using B3LYP levels. Molecular electrostatic potentials (MEP) and Density of states (DOS) were calculated by B3LYPlevel at 6-31G (d,p) basis set. A Potential Energy distribution of the g-CN molecule is also calculated by VEDA program.

3. RESULT AND DISCUSSION

3.1. Structural and Morphological Analysis

The phase structures of the samples were investigated by XRD. Fig.1.a shows the XRD pattern of graphitic carbon nitride nanoparticles. The strongest sharp reflection peak at the position of 2θ=27.4° can be assigned to the (002) diffraction of *g*-C3N4, which confirms the formation of a Hexagonal graphitic structure. A low-angle (100) peak at around 15.3° corresponding to the tri-s-triazine units packing in the lattice planes parallel to the c-axis, peak presumably relates to an in-plane structural packing motif, such as the hole-to-hole distance [8]. The crystallite sizedetermined using Debye-Scherer formula is around 36 nm.SEM micrograph shows that the prepared samples consist of an assembly of hexagonal nano flake like structure.

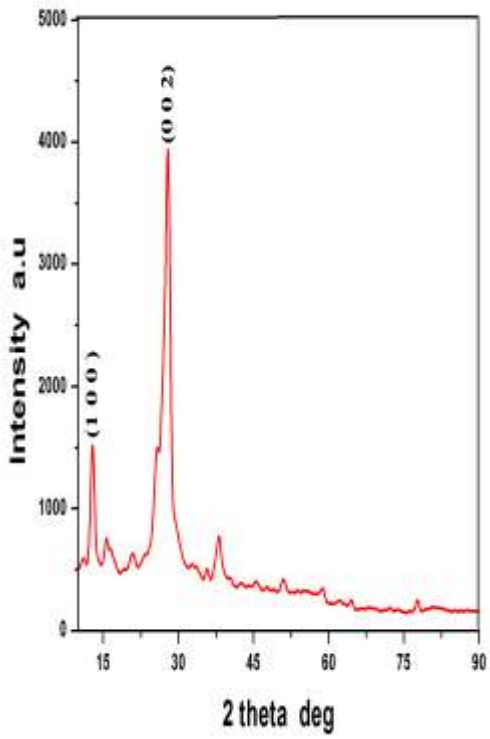

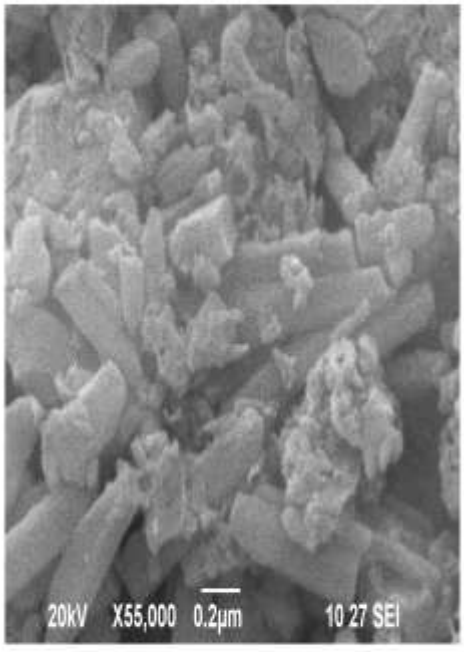

Fig.1.a XRD pattern of g-CN nanoparticle **Fig 1.b. SEM micrograph of g-CN**

3.2. Geometrical Parameters:

The optimized molecular structure parameters such as Bond length, Bond Angle and Dihedral angles were calculated by B3LYP G31-6G(d,p) basis set are shown in table1. In accordance with atomic numbering structure of the g-CN molecules is present in Fig (2.b) To the Best of our knowledge there is no experimental Bond Angle, Bond length and Dihedral Angle of the g-CN molecule was reported. In g-CN molecule, only carbon and nitrogen atoms are present. From the title molecules, C-N bond distance is calculated in the ring structure molecules [10]. The calculated Bond length of the title molecule is in the range of 1.23 to 1.49Å. The Bond angle of the g-CN molecular element (N-C-N) bonding varies in the range of 111.96 -154.76 degree and (C-N-C) bonding Angle is in the range of 104.36 – 124.58 degree.

ISSN 2321-807X
Volume 13 Number6
Journal of Advances in chemistry

Table 1: Theoretically calculated Bond Angle, Bond length and Dihedral Angle of optimized structure. of g-CN molecule

Parameter	B3LYP /6-31G (d, p)	Parameter	B3LYP /6-31G (d, p	Parameter	B3LYP /6-31G (d, p)
Bond length(A°)					
C1-N9	1.2462	N8-C3-N13	120.7778	N8-C2-N7-C6	167.1331
C1-N12	1.4452	N9-C3-N13	124.4748	N14-C2-N7-C6	-13.8529
C1-N14	1.463	N10-C4-N11	121.1533	N7-C2-N8-C3	-170.9108
C2-N7	1.4766	N10-C4-N14	121.2855	N14-C2-N8-C3	10.1982
C2-N8	1.2497	N11-C4-N14	117.5133	N7-C2-N14-C1	-167.4157
C2-N14	1.4486	N11-C5-N12	154.7178	N7-C2-N14-C4	3.4575
C3-N8	1.491	N7-C6-N10	141.4599	N8-C2-N14-C1	11.5881
C3-N9	1.4389	C2-N7-C6	111.0602	N8-C2-N14-C4	-177.5388
C3-N13	1.225	C2-N8-C3	116.0735	N9-C3-N8-C2	-34.3786
C4-N10	1.3153	C1-N9-C3	117.0174	N13-C3-N8-C2	141.2638
C4-N11	1.3972	C4-N10-C6	109.2289	N8-C3-N9-C1	36.5668
C4-N14	1.3921	C4-N11-C5	104.3129	N13-C3-N9-C1	-138.8913
C5-N11	1.2374	C1-N12-C5	106.4052	N11-C4-N10-C6	164.3707
C5-N12	1.2087	C1-N14-C2	112.5997	N14-C4-N10-C6	-13.0477
C6-N7	1.2297	C1-N14-C4	124.5823	N10-C4-N11-C5	178.8802
C6-N10	1.3123	C2-N14-C4	122.1262	N14-C4-N11-C5	-3.6073
Bond angle (°)		**Dihedral angle(°)**		N10-C4-N14-C1	-178.9269
				N10-C4-N14-C2	11.3187
N9-C1-N12	123.8461	N14-C1-N9-C3	-14.6626	N11-C4-N14-C1	3.564
N9-C1-N14	124.0186	N9-C1-N12-C5	176.7242	N11-C4-N14-C2	-166.1904
N12-C1-N14	112.1229	N14-C1-N12-C5	-4.5174	N12-C5-N11-C4	-2.7122
N7-C2-N8	123.5718	N9-C1-N14-C2	-9.5838	N11-C5-N12-C1	7.2909
N7-C2-N14	111.9643	N9-C1-N14-C4	179.8067	N10-C6-N7-C2	15.3695
N8-C2-N14	124.456	N12-C1-N14-C2	171.6603	N7-C6-N10-C4	-1.1127
N8-C3-N9	114.5903	N12-C1-N14-C4	1.0508		

ISSN 2321-807X
Volume 13 Number6
Journal of Advances in chemistry

3.3 Molecular electrostatic potential studies

From this study, it is observed that the electron density and electrostatic potential plot have been mapped for g-CN molecule. The molecular electrostatic potential (MEP) at a point *r* in the space around a molecule (in atomic units) can be expressed as

$$V(r) = \sum Z_A \ |R_A - r| - \int \rho(r')/|r'|$$

Where, ZA is the charge on nucleus A, is the electronic density function for the molecule [11]. The first and second terms represent the contributions to the potential due to nuclei and electrons, respectively. V(r) is the resultant at each point *r*, which is the net electrostatic effect produced at the point *r* by both the electrons and nuclei of the molecule.

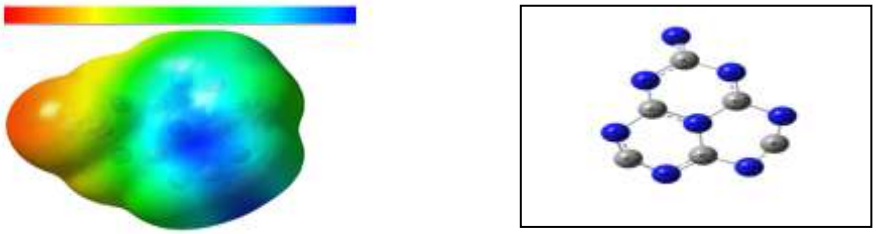

Fig 2a,b: Molecular electrostatic potential and Molecular orbital diagram of g-CN molecule

In the MEP plot blue colour shows nucleophilic and red colour shows electrophilic potentials [12]. The electron density map of the title of the molecules shows the uniform distributions from electropositive to the electronegative region. Negative electron density value of the g-CN molecule is -0.05931 (A) and positive electron density value is 0.05931(A). The electrostatic potential regions corresponding to the attraction of proton by the electron density of the molecules just as like as a lone-pair π bond [14]. The positive electrostatic potentials correspond to the repulsion of protons by nuclear regions. Red colour indicates the strong repulsions and it is present in N atom of g-CN molecule. Blue colour indicates the strong attraction and it is observed for few C atoms and center of the ring formed by N and C atoms. From this study, it is observed that the electrophilic potential is predominated in the title molecule because of the lone-pair exist in the N atom of the g-CN molecule.

3.4 UV-Visible, HOMO-LUMO and DOS Studies

3.4.1 UV-Visible Spectrum Analysis

The TD-DFT was used to determine the low lying excited state of g-CN molecule on the basis of optimized Ground state structure [13]. The excitation energy, Absorption wavelength and oscillation strength have been carried out and compared with experimental data. The electronic transition calculation have been performed in the water solutions using PCMR/non-symmetric T matrix model by TD-DFT/B3LYP and HF method [14]. The UV-Visible spectrum of g-CN molecule is shown in fig (3.a). The strong blue shift in the UV– Visible absorption region (312 nm) confirms the nano dimensional state of g-C_3N_4 nano particles. The electronic transition is predicted at 360,372 and 549 nm and its corresponding oscillation strength were 0.4444, 0.0022 and 0.0007 respectively. The experimental wavelength at 312 nm in water solution is shown in fig (3.a.)

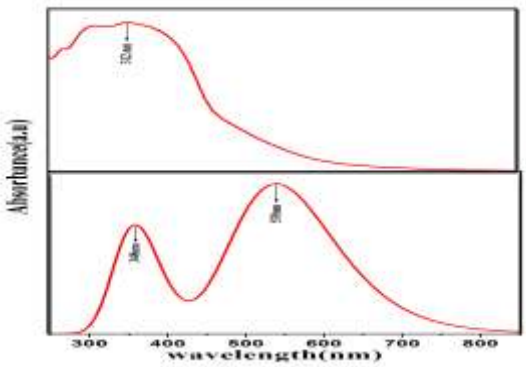

Fig 3.a Theoretical and Experimental UV-Visible Spectrum of g-CN molecule

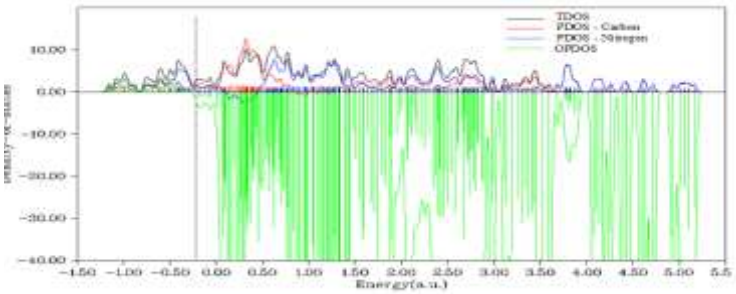

Fig 3.b: Optimized DOS, PDOS and TDOS of the g-CN molecule

ISSN 2321-807X
Volume 13 Number6
Journal of Advances in chemistry

Table 2: Experimental and computed absorption wavelength λ (nm), excitation energies E and oscillator strength (f) ofg-CN using TD-HF and B3LYP /6-31G (d, p) method

Transition level	Wavelength (λ)		Energy (eV)		Oscillation strength (f)	
	Experimental	Theoretical				
		HF	B3LYP	HF	B3LYP	HF	B3LYP
I	312	539	308	2.3021	0.4108	0.0068	0.0024
II		366	816	3.3844	1.4176	0.0019	0.003
III		353	716	3.5117	1.7308	0.0032	0.0369

3.4.2 DOS Studies

Density of states of the g-CN molecule is shown in fig.(3.b) the density of states graph has been plotted from -1.5 a.u to 5.5 a.u. the Partial density of state of the g-CN molecule dominate in the LUMO region than the DOS. But, the DOS of the C atom is lower than the TDOS of the given molecule. The DOS of the N atom is more dominated in the LUMO region than the HOMO region up to the range of energy – 5 a.u. Electron density of the nitrogen atom of the given molecule is dominated in the HOMO region than the electron density of C atom [15]. PDOS is higher in LUMO region than in HOMO region.

3.4.3 HOMO – LUMO Studies

The HOMO-LUMO is named as frontier molecular orbitals, which play a vital role in electronic, optical properties and energy band-gap of the HOMO-LUMO [16]. The HOMO-LUMO energy is used to study the molecular chemical stability, Hardness and softness of the molecules. The HOMO shows that the localized charge density is higher for the lone-pair of Nitrogen atom than the other C-N atoms in the molecules.

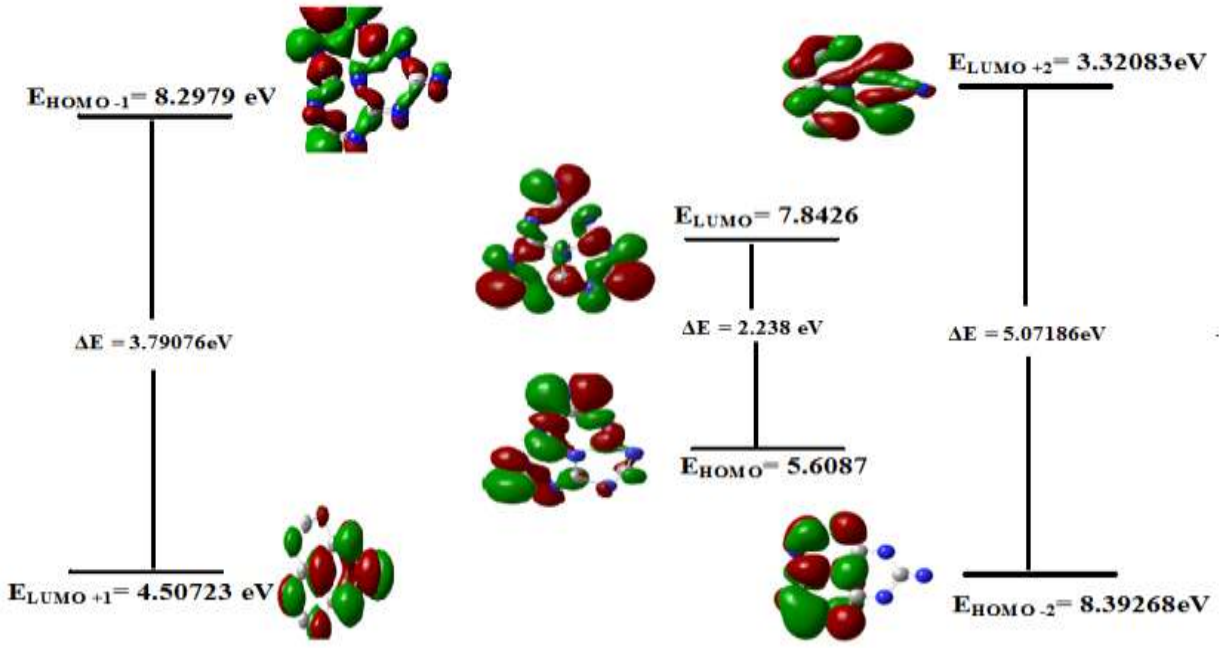

Figure 4: Frontier orbital diagram of g-CN molecule

The LUMO shows that the charge density is localized in the N7-C6-N10 and it is higher than the other atom in the title of the molecule. The calculated band gap energy of HOMO-LUMO is 2.239eV which is in good agreement with the measured experimental Eg of title of the molecule that is equal to 2.78eV. The Energy of the HOMO-LUMO is directly related to the Ionization potential energy and electron affinity [17]. It is observed that the energy of the LUMO is just higher than the HOMO. Therefore the electron affinity of this molecule is just higher than the Ionization potential.

Table 3: Calculated HOMO and LUMO and Frontier orbital of g-CN by B3LYP /6-31G (d, p) method

Energy State	MO Energy	Energy State	MO Energy	ΔE
HOMO	7.84738	LUMO	5.60873	2.23865
HOMO	7.84738	LUMO+1	4.50723	3.34015
HOMO	7.84738	LUMO+2	3.32083	4.52655
HOMO-1	8.29799	LUMO+1	4.50723	3.79076
HOMO-2	8.39268	LUMO+2	3.32083	5.07186

3.5 Vibrational Analysis

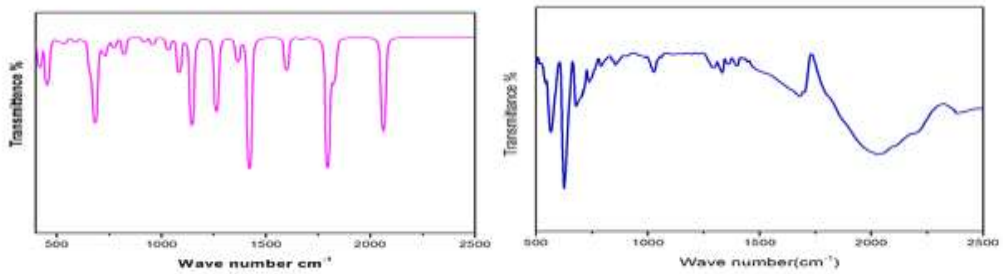

Fig.5a&b: Theoretical and Experimental IR spectrum

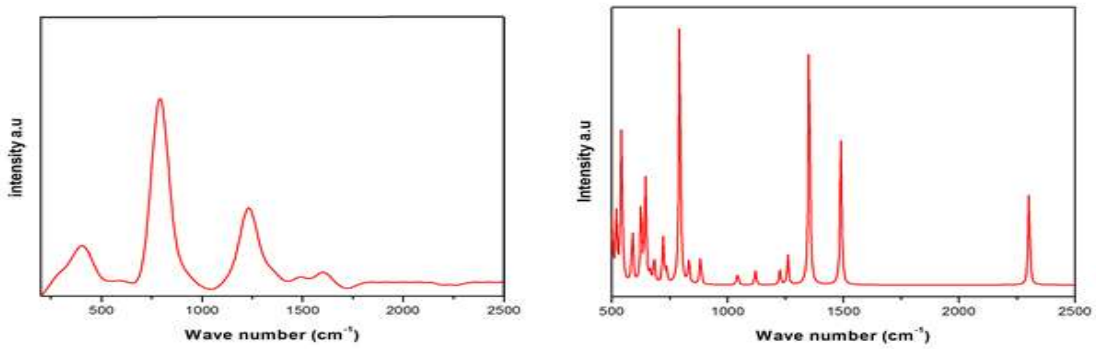

Fig 6.a&b Experimental and Theoretical Raman spectrum of g-CN

3.5.1 C-N, C=N Stretching mode

The experimental and computed FT-IR and FT-RAMAN spectrum were shown in figure (5a,b& 6a,b).The deductions of C-N vibrations are very difficult task because it is mixing several bands in these regions [18]. The C-N stretching absorption in the range of 1080 cm^{-1} to 1360 cm^{-1} corresponds to aromatic compounds [19]. From the literature survey, C-N stretching vibration present at 1335 cm^{-1} for 2,4 – dinitrophenyl hydrazine and 1368 cm^{-1} for Benzamide [20]. In our present work, g-CN shows predominant peak at 1026 cm^{-1} and 1334 cm^{-1} in IR spectra and 1232 cm^{-1} in Raman spectra have been assigned to C-N stretching vibrations. Theoretically computed values of C-N stretching vibrations at 1042 cm^{-1} and 1366 cm^{-1} show good agreement with experimental values. The C=N Stretching vibrations are present in the range of 1692 cm^{-1}, 1640 cm^{-1}. In our theoretical calculation at 1607 cm^{-1} by B3LYP method, it is assigned to C=N stretching vibration. However, the recorded Laser Raman spectral band shows a strongest peak at 1605 cm^{-1}. This is in good agreement with the Theoretical values.

3.5.2 C-N-C and N-C-N Bending mode

The IR spectral band was recorded at 2032 cm^{-1} is assigned to anti-symmetric C=N stretching vibrations found by Gaussian visualisation software. But there is no reference for C=N anti-symmetric stretching vibrations. The Nitrosol groups spectrum present at 2100 – 2270 cm^{-1}. But g-CN molecule consist of aromatic amine group structure, it has only C-N, C=N bonding were found [21]. From the theoretically calculated spectrum, Medium peak is present at 1983 cm^{-1} and it is assigned to asymmetric stretching of C=N vibrations using Gauss view visualisation program. This theoretical value is coinciding at 2032 cm^{-1}in the experimental IR spectral line. So that the theoretical and experimental values asymmetric stretching C=N vibrations are in partially coincide with to each other [22]. In the case of g-CN, vibrations involving the C-N in plane bending were found throughout the theoretically computed region from 633 cm^{-1} to 992 cm^{-1} as shown2in table. These are matched well with the experimental spectral band at 624 cm^{-1}, 673 cm^{-1}, 734 cm^{-1} and 850 cm^{-1} for IR spectrum and 787 cm^{-1} for Raman spectrum respectively. The Aromatic g-CN structure shows that the Torsional modes appear in the lower wave number regions [23]. In our case, the calculated normal mode vibrations below 600 cm^{-1}wave number are mainly the Torsional modes.

Table 4: Experimental and computed Wave number, IR and Raman intensities and Vibrational Assignments of g-CN using B3LYP /6-31G (d, p) method

S.No	Wave number (cm-1)			Intensity			PED (<10%)
	Exp IR	Exp. RAMAN	B3LYP/6-31G(d,p)	Exp IR	Exp Raman	B3LYP/6-31G(d,p)	
1			56			2.44	(T) N13 - C3 - N8 - C2 (29%) + (T) C1 - N14 - C2 - N7 (26%)
2			106			4.79	(T) N13 - C3 - N8 - C2 (24%) + (T) C6 - N10 - C4 - N11 (13%)
3			154			3.61	(T) C1 - N12 - C5 - N11 (50%)
4			165			2.50	(T) C6 - N7 - C2 - N8 (13%) + (T) N7 - C6 - N10 - C4 (33%)
5			211			7.93	(T) C4 - N14 - C2 - C1 (50%)
6			310			36.57	(B) C2 - N7 - C6 (10%) +(B) N13 - C3 - N8 (21%)
7			366			3.35	(B) C1 - N12 - C5 (13%) + (B) N13 - C3 - N8 (14%)
8		403	402		247.74	84.78	(B) N13 - C3 - N8 (38%)
9			436			134.13	(S) C1 - N14 (13%) + (T) N11 - C5 - N12 - C1 (12%)
10			450			6.88	(S) N9 - C1 (13%) +(B) N12 - C5 - N11 (30%)
11			489			9.29	(B)N7 - C6 - N10 (12%) + (T)N12 - C5 - N11- C4 (15%)
12			501			2.66	(B)C6 - N10 - C4 (15%) + (B)N7 - C2 - N8 (12%)
13			517			15.51	(B)N7 - C2 - N8 - N14 (13%) +(T) N11 - C5 - N12 - C1 (19%)
14			547			0.83	(B)N11 - C5 - N12 (24%) + (T)N10 - C6 - N7 - C2 (22%)
15	558		565	5.29		11.41	(T)N9 - C1 - N12 - N14 (29%) + (T)N13 - C3 - N9 - N8 (27%)
16			599			3.76	(T)C5 - N11 - C4 - N10 (17%) +(T) N14 - C2 - N7 - N8 (23%)
17	624		633	9.07		83.93	(S)N10 - C4 (13%) + (T)N10 - C4 - N14 - N11 (15%)

ISSN 2321-807X
Volume 13 Number6
Journal of Advances in chemistry

Table 4. continuation

S.No	Wave number (cm-1)			Intensity			PED (<10%)
	Exp IR	Exp. RAMAN	Exp IR	Exp. RAMAN	Exp IR	Exp. RAMAN	
18			657			243.53	(B)N10 - C6 - N7 (13%) + (B)C1 - N9 - C3 (19%)
19	673		675	3.48		10.82	(T)N9 - C3 - N8 -N13 (23%) + (T)N11 - C4 - N14 - N10 (13%)
20			725			33.81	(T)N12 - C1 - N9 -N14 (12%) +(T) N14 - C2 - N8 - N7 (21%)
21			710			16.85	(B)N8 - C2 - N7 (13%) + (B)N7 - C6 - N10 (23%)
22	734		742	1.92		28.05	(B)N11 - C5 - N12 (11%) +(S) C3 - N8 (12%) +(S) C2 - N7 (38%)
23		787	789		474.17	48.68	(B)N11 - C5 - N12 (14%) +(B) N14 - C1 - N9 (28%)
24	850		882	0.817		13.40	(S)C2 - N7 (23%) + (B)N12 - C1 - N9 (10%)
25			921			21.27	(S)C3 - N9 (43%) + (S)C1 - N12 (33%)
26			992			35.64	(S)C2 - N14 (21%) +(S) C4 - N11 (29%) +(B) N7 - 2C - N8 (15%)
27	1026		1042	1.43		100.20	(S)C6 - N7 (25%) + (B)N9 - C1 - N14 (20%)
28			1102			253.30	(S)N14 - C1 (17%) + (S)N10 - C4 (21%) + (B)C5 - N11 - C4 (28%)
29		1232	1214	305.72		218.50	(S)C4 - N14 (27%) + (B)N9 - C1 - N14(22%)
30	1290		1312	1.02		64.10	(S)C5 - N11 (28%) +(S) C2 - N8 (45%)
31	1334		1366	1.47		384.70	(S)C4 - N10 (54%) + (B)N11 - C4 - N14 (16%)
32			1537			96.02	(S)C2 - N8 (15%) + (S)C6 - N7 (58%)
33		1605	1607		206.74	5.86	(S)C1 - N9 (13%) + (S)C4 - N10 (61%)
34			1726			372.86	(S)C6 - N7 (31%) + (S)C1 - N9(41%) +(S) C3 - N13 (12%)
35			1756			116.64	(S)C6 - N7(29%) + (S)C2 - N8 (20%) + (S)C3 - N13 (23%)
36	2032		1983	2.98		279.14	(S)C5 - N11(55%) + (S)C5 - N12(39%)

3.6 Dipole Moment and Hyper polarizability

The hyper polarizability (β) of optimized geometrical structure of g-CN molecule and related polarizability (α) are calculated using TD-DFT/HF and B3LYP6-31G (d,p) basis set. The hyper polarizability of the title molecule is related to be β, Polarizability α and Δα based on the finity field of approach is represented as [23, 26].

$$\mu = (\mu^2_x + \mu^2_y + \mu^2_z)^{1/2}$$

$$\Delta\alpha = 1/\frac{1}{\sqrt{2}}[(\alpha_{xx} - \alpha_{yy})^2 + (\alpha_{yy} - \alpha_{zz})^2 + (\alpha_{zz} - \alpha_{xx})^2 + 6\,\alpha^2_{xx}]^{1/2} \quad \& \quad \alpha_{tot} = \alpha_{xx} + \alpha_{yy} + \alpha_{zz} / 3$$

$$\beta = [(\beta_{xxx} + \beta_{xyy} + \beta_{xzz})^2 + (\beta_{yyy} + \beta_{xxy} + \beta_{yzz})^2 + (\beta_{zzz} + \beta_{xxz} + \beta_{yyz})]^{1/2} \quad \& \quad \beta = (\beta^2_x + \beta^2_y + \beta^2_z)^{1/2}$$

From this study, dipole moment, polarizability and hyper polarizability were calculated using the perturbation theory in tensor matrix. The dipole moment of the g-CN molecule is used to investigate inter-molecular interaction. It is stronger for high value of dipole moment [24]. The dipole moment of the title of the compound is calculated using TD-DFT/HF and B3LYP method and its values are 12.8637 Debye and 6.6863 Debye. The total polarizability of the title molecule is calculated using TD-DFT/HF and B3LYP method and its values are -265.93 $x10^{-32}$esu and -262.80 $x10^{-32}$esu. The Hyper polarizability of g-CN molecule is calculated using TD-DFT/HF and B3LYP are 16.891$x10^{-32}$esu and 5.704$x10^{-32}$esu. The first order hyper polarizability of title molecule calculated by TD-DFT/HF is found to be approx. 4.3 times greater than urea and 1.48 times greater than urea by B3LYP method [25]. This result clearly shows that the title molecule has NLO properties.

Table 5: Theoretically calculated Polarizability α and hyper polarizability β of g-CN using TD-DFT/HF and B3LYP /6-31G (d, p)

α & β components	HF/6-31G(d,p)	B3LYP/6-31G(d,p)
α_{xx}	-112.461	-106.5369
α_{yy}	-71.175	-75.4376
α_{zz}	-76.945	-74.6059
α_{xy}	2.244	-1.8087
α_{xz}	-4.6966	-3.5491
α_{yz}	-0.6537	-0.8655
α(total)	-265.93 $x10^{-32}$esu	-262.80 $x10^{-32}$esu
β_{xxx}	-110.7441	-51.2827
β_{yyy}	-2.3302	19.2956
β_{zzz}	-1.8975	-1.1405
β_{xyy}	-47.8152	-24.1844
β_{xxy}	-1.7129	8.0898
β_{xxz}	-29.7267	-18.7663
β_{xzz}	-8.0717	-4.8966
β_{yzz}	1.2546	1.8781
β_{yyz}	4.9954	5.0782
β_{xyz}	0.4612	-0.0974
β (total)	-16.9807 $x10^{-32}$esu	5.7053 $x10^{-32}$esu

Table 6: Theoretically calculated Dipole moment (μ) of g-CN using TD-DFT/HF and B3LYP/6-31G (d, p)

μ value	HF/6-31G(d,p)	B3LYP/6-31G(d,p)
μ_x	-12.7842	-6.1972
μ_y	-0.1984	2.4479
μ_z	-1.3231	-0.5557
μ	12.8637	6.6863

3.7 Natural Bonding Orbital Analysis

The NBO analysis were performed by Gaussian 09 software package at the basis set of TD-DFT/HF and B3LYP 6-31 G (d,p). NBO analyses provide the acceptor and donor interaction of the title molecule based on second order perturbation of Fock matrix. The NBO calculations used to measure the intermolecular delocalization of the atoms. The NBO analyses was used to determine the most accurate possible natural Lewis structure and also to calculate the percentage of the electron density of all orbitals [26]. The interaction result depends on losses of density of electron from the localized Lewis structure into the empty non-lewis structure [27]. The stabilization Energy of each donor and acceptor is associated with delocalisation. The stabilization Energy calculated as

$$E(2) = \Delta E_{ij} = q_i \frac{F(i,j)^2}{\varepsilon_j - \varepsilon_i}$$

Generally, the stabilisation Energy E(2) value is high for more intensive interaction between electron donor and acceptor and it is clearly shows that more charge transfer conjugate interactions in the molecular system from g-CN molecule, the interaction between Bonding (C6-N7) and anti-bonding (C6-N10) give strong stabilization energy of 234.41 and 133.03 respectively. It is noted that the occupancies of (C-N) bonding of g-CN molecule obtained in the range of (1.989 – 1.553). Therefore the result suggests that C-N bondings are essentially controlled by 'P' character of the hybrid orbitals [28]. The N atom of the g-CN molecule is donating electron from LP – N14 to (C4-N11) show the high stabilization energy of 65.5 Kcal/mol and LP N10 to (C4-N14) interaction has less stabilization energy of 13.45 Kcal/mol.

The Bonding (C3-N8) and anti-bonding (C2-N7) intermolecular interactions has the less stabilization energy and it is 10.14 KJ/mol. The strong intra molecular conjugate interaction of the σ and π electron of bonding C-N to the anti-bonding C-N in the ring lead to the stabilization of the g-CN molecules as an evidence from the table(5). From this study, N lone-pair (N14) show the lowest occupancy value and is 1.610 a.u and high energy is 0.365 a.u. The Natural population analyses were also calculated for g-CN molecule. From this study, it is shown that the general quality of the Natural Lewis structure is about 94.19%, non-Lewis structure is 5.54% and Rydbeck non-Lewis structure is 0.27% of the g-CN molecule.

Table 7: Second Order Perturbation Theory analysis of Fock matrix in Natural bonding orbital of GCN calculated by B3LYP /6- 31-G (d,p)method

Donor NBO(i)	ED/e	Acceptor NBO(j)	ED/e	E(2) kcal/mol	E(j)-E(i) a.u	F(i,j) a.u
σ C 3 - N 8	1.91831	σ * C 2 - N 7	0.2389	10.14	0.97	0.089
σ C 4 - N 11	1.8999	LP* C 5	0.13679	24.21	0.66	0.132
π C 4 - N 11	1.6707	LP* C 5	0.10275	14.22	0.18	0.05
π C 4 - N 11	1.98731	σ *C 5 - N 12	0.35301	64.24	0.34	0.133
π C 5 - N 12	1.9895	σ * C 1 - N 9	0.02211	15.13	0.43	0.075
π C 6 - N 7	1.63997	π* C 2 - N 8	0.23837	31.42	0.2	0.073
σ C 6 - N 7	1.98476	σ * C 6 - N 10	0.30012	234.41	0.74	0.377
σ C 6 - N 10	1.97324	σ * C 4 - N 11	0.59919	133.03	0.14	0.125

σ C 6 - N 10	1.5241	π* C 6 - N 7	0.03055	92.36	0.8	0.266
LP(1) N 8	1.85479	σ * C 2 - N 14	0.09344	19.47	0.67	0.103
LP(1) N 9	1.83832	σ * C 1 - N 14	0.10275	21.16	0.63	0.105
LP(1) N 10	1.82464	π* C 4 - N 14	0.06627	13.45	0.74	0.092
LP(1) N 12	1.7409	LP* C 5	0.01397	31.78	0.26	0.09
π N 13	1.97343	LP* C 3	0.0165	16.08	1.31	0.13
LP(1) N 14	1.60652	σ * C 2 - N 8	0.01568	27.03	0.34	0.089
LP(1) N 14	1.6099	σ * C 4 - N 11	0.05342	65.5	0.23	0.115
σ* C 2 - N 7	1.87819	π* C 3 - N 8	0.13679	19.01	0.03	0.064
π* C 4 - N 11	1.8999	π* C 5 - N 12	0.01751	36.54	0.08	0.069
π* C 5 - N 12	1.90508	π* C 1 - N 9	0.24676	28.45	0.03	0.048
π C 6 - N 10	1.5535	LP* C 6	0.01218	22.76	0.35	0.202

4. CONCLUSION

The metal free polymeric graphitic carbon nitride was successfully synthesized by thermal pyrolysis method. The complete molecular structural parameters of optimized geometry of g-CN have been reported using DFT calculations. Computed geometrical parameters were compared with observed XRD data.The calculated vibrational frequencies have been compared with the experimentally recorded values. It is found that scaled vibrational assignments are in good agreement with experimental values of FT-IR and Raman spectra. Decrease in the theoretically computed HOMO–LUMO energy gap value has substantial influence on the intra-molecular charge transfer of the molecule. Electronic stabilization of g-CN was discussed by NBO analysis by means of donor and acceptor orbital interactions.The hypothetical computation of hyperpolarizability is extremely valuable to show the bearing of charge delocalization.

References:

1. T. Karakurt, M. Dinc¸ er, A. C¸ etin, M. Sekerci, Spectchim. Acta 77A (2010) 189–198.
2. M. Silverstein, G.C. Basseler, C. Morill, Wiley, New York, 1981.
3. J. Tonannavar, J. Yenagi, V.B. Veena sangeeta Sortur, M.V. Jadhav, Kulkarni, Spectrochim. Acta A 77 (2010) 351–358.
4. L.X. Hong, G.X. Yang, Z.X. Zhou, Comp. Theor. Chem. 976 (2011) 191–196.
5. P. Sett, T. Misra, S. Chattopadhyay, A.K. De, P.K. Mallick, Vib. Spectrosc. 44 (2007) 331–342.
6. M. K. Cyranski, A. Jezierska, P. Klimentowska, J. J. Panek, G. L. Zukowska, A. Sporzynski, *J. Chem. Phys.* 2008, *128*, 124512.
7. Gracia J, Kroll P: J Mater chem 2009, 19:3020.
8. D.M. Teter, R.J. Hemley, Sceince 271 (1996) 53.
9. S. Suresh, S. Gunasekaran, S. Srinivasan, Spectro chim. Acta 132A (2014) 130–141.
10. S. Sebastian et al. Spectro chimica Acta Part A: Molecular and Biomolecular Spectroscopy, 136 (2015) 1107–1118.
11. Lee. Y, et al. J. Phys. Chem. C 111, 1042 -1048 (2007).
12. Ren Y M, Yan N, Feng J, et al. Mater ChemPhys, 2012,136: 538−544
13. Sun Y B, Chen C L, Tan X L, et al. Dalton T, 2012, 41: 13388−13394
14. Zhang K, Kemp K C, Chandra V. Mater Lett, 2012, 81: 127−130
15. Liu X J, Pan L K, Zhao Q F, et al. Chem Eng J, 2012, 183: 238−243
16. Deng S Z, Tjoa V, Fan H M, et al. J Am ChemSoc, 2012, 134: 4905–4917
17. An X Q, Yu J C, Wang Y, et al. J Mater Chem, 2012, 22: 8525−8531
18. Silverstein M., Spectrometric identification of Organic compound, 1982.
19. Shanmugam R, Spectra chemActa: Part A , 1984, 762.
20. Zhang, Z.; Leinenweber, K.; Bauer, *J. Am. Chem. Soc*. 2011, *123*, 7788.
21. Hui Pan, Yong-Wei Zhang; Nanoscale Research Letters 2011, 6:97.
22. V. Balachandran, S. Rajeswari, S. Lalitha, J. Mol. Struct. 1007 (2012) 63–73.
23. Zhang N, Yang. M.Q, Liu. S. Chem. Rev. 2015, 115, 10307−10377.
24. Yang. J, Wang. D, Han, H.; Li, C. Acc. Chem. Res. 2013, 46, 1900−1909.
25. Tu. W, Zhou. Y. Adv. Funct. Mater. 2013, 23, 4996−5008.
26. Fan. W, Zhang. Q, Wang. Y. Phys. Chem. Chem. Phys. 2013, 15, 2632−2649.
27. J. Guan, S. Y. Zhang, S. H. Liu, et.al., Chem. Soc., 2015,137, 6152-6155.
28. A. Frish, A.B. Nielson, A.J. Holder, GASSVIEW view, Gaussian Inc., 2000.